BAMBOO METALLIZATION FOR AESTHETIC FINISHING OF FURNITURE AND WOOD DECORATIVE OBJECTS BY AN ELECTROLESS/ELECTROLYTIC PROCESS

José de Jesús Pérez Bueno†*

Researcher/Dr.
E-mail: jperez@cideteq.mx

Maria de Lourdes Montoya García

Researcher/M.C.
Centro de Investigación y Desarrollo Tecnológico en Electroquímica, S.C.
Parque Tecnológico Querétaro Sanfandila
Pedro Escobedo 76703, Mexico
E-mail: lmontoya@cideteq.mx

Maria Luisa Mendoza López

Researcher/Dra.
Tecnológico Nacional de México
Instituto Tecnológico de Querétaro
Av. Tecnológico s/n Esq. Mariano Escobedo, Col. Centro
Querétaro 76000, Mexico
E-mail: mluisaml@yahoo.com

Gabriela Montoya García

Industrial/Ms.
Mueblería Montoya
Aguascalientes, México
E-mail: gaby_montoya2000@yahoo.com.mx

(Received September 2018)

Abstract. This work aims to propose and describe bamboo metallizing, in part or totally, for furniture or aesthetical decorations. Bamboo provides a diverse metallic appearance; however, its use with real metal, already conferred to plastics, may increase the chance of use of this green material. The furniture industry requires sustainable options for both the base material for manufacturing of many pieces of furniture with a useful purpose, and surfaces finished with high quality and variety in their aesthetic appearance. This includes bamboo ornaments, which are useful to complement interior decoration. The coatings obtained include copper, silver, nickel, brass, and tin, each of which had some variants in luster. The main change incorporated into the process for metallizing nonconducting surfaces was the introduction of a common base for all surfaces, regardless of its roughness, shape, size, or other surface conditions. Then, this base was taken through an electroless process followed by electrolytic stages. Modification of the current process prevents the need for an initial stage of etching to increase chemical conditioning and roughness. The obtained metallic luster was that intended for decorative applications.

Keywords: Bamboo, furniture, sustainability, finishing, coatings, veneer.

INTRODUCTION

The furniture industry requires both the base material for the manufacturing of furniture with useful purpose and surface finishing with high quality and variety in their aesthetic properties. Bamboo has been in use for centuries, but now it is considered one of the few sustainable materials used in construction and other traditional uses of wood (Obataya et al 2007). Bamboo is considered

* Corresponding author
† SWST member

Wood and Fiber Science, 51(2), 2019, pp. 144-159
https://doi.org/10.22382/wfs-2019-016

an outstanding material for its mechanical properties but mainly as a sustainable material, which is gaining popularity in applications usually devoted to diverse woods or even to metals (Eichhorn et al 2010). Also, its use in interior decoration is rising in importance, which includes wood-made objects and even some bamboo ornaments that could be used to complement indoor designs. Surface finishing of bamboo has progressed from simply dried surfaces to using countless varieties of paints and lacquers with dyes or abrasion-resistant particles adjusted for the many applications.

Surface modification of materials confers an external finishing that fulfills the required characteristics for their intended use. Currently, metallization of plastics such as Acrylonitrile-Butadiene-Styrene ABS has been applied to have, at the same time, lightweight and low production cost, as well as an aesthetic metallic appearance. The most frequent plating finishes are with nickel, chrome, copper, silver, gold, and brass. Metallization of nonconducting surfaces is achieved mainly by using chemical procedures (Sun et al 2012). The electroless technique grows a homogeneous conducting thin film in the absence of an external electrical current (Sittisart et al 2014; Zhao et al 2014). Among the many stages of the electroless process, pretreatment and activation are of major concern because of the hazardous chemical composition and cost of palladium, respectively. Preconditioning of the surface is crucial for the quality of the final metallic deposit. The surface condition affects the allocation of sites during activation and determines the feasibility for plating. After the creation of an autocatalytic conductive metallic thin film, one or more layers are electrolytically deposited, thereby increasing the thickness, which confers mechanical resistance and the metallic appearance.

Metallization of nonconducting surfaces such as wood, paper, plastics, and fabrics has been achieved by using a chitosan layer on the substrates and then activating by implantation of metallic ions, which is favorable because of their affinity to chitosan amine groups (Wang et al 2011; Shi et al 2017; Zhao et al 2018). Electromagnetic interference shielding is of importantance in metallizing wood (Sun et al 2012; Hui et al 2014), which is frequently accompanied by seeking to obtain self-cleaning performance (Xing et al 2018). Nonetheless, using a layer before activation with metallic ions of palladium, palladium/tin, tin, or other possible alternatives is an open subject. The difficulty lies in the porosity and adsorption capacity, which prevents the use of conventional methods that imply dipping into a chemical bath that changes the wood and leaves residues inside.

The aim of this work was to propose metallizing, in part or totally, of bamboo for furniture or aesthetic decorations, and the procedure to do so. Bamboo provides diverse metallic appearances; however, its use with real metal, already conferred to plastics, may increase the chance of use of this green material. The furniture industry requires sustainable options for both the base material for manufacturing of many pieces of furniture with useful purposes and surfaces finished with high quality and variety in their aesthetic appearance. This includes bamboo ornaments useful for complementing interior decoration.

MATERIALS AND METHODS

The culms of bamboo *Guadua angustifolia* of about 6-8 yr old were used. The top and lowest bottom zones of the culms were not used. The vascular bundles, epidermis, phloem, protoxylem, metaxylem vessels, fiber, and cortical parenchyma did not vary significantly among the samples (Xing-yan et al 2015).

The process steps include 1) natural bamboo conditioning (cutting, cleaning, and dehydration), 2) preserving bamboo, 3) bamboo dehydration, 4) applying lacquer, 5) drying, 6) application of colloidal copper, 7) drying, 8) surface activation, 9) rinsing, 10) electroless process for metallic coverage, 11) rinsing, 12) electrolytic process (nickel, chrome, brass, etc.), 13) rinsing, 14) draining and drying, and 15) placement on the design of a furniture or decorative object. Table 1

Table 1. Process used for metallizing nonconducting surfaces of bamboo.

Stage	Vol. (L)	Material	Immersion time	Temperature	Comments
Bamboo preparation	—	Bamboo and wire	—	—	—
Bamboo preserving	—	$H_3BO_3/Na_2B_4O_7 \cdot 10H_2O/H_2O$) 1:1:50	24 h	—	—
Bamboo dehydration	—	—	Min. 5 h, max. 24 h	80-90°C Furnace	—
Lacquer	—	Varnish and thinner	Three layers Airbrush painting or immersion (min. 3 s)	—	—
Drying	—	—	Max. 30 min	RT or max. 40°C	—
Cu plating	—	Cu paint	Three layers Airbrush painting or immersion (min. 3 s)	—	—
Drying	—	—	Max. 30 min	RT or max. 40°C	—
Surface activation	4.5	$(SnCl_2)$/HCl/deionized water	Max. 5 min	RT	Mechanical stirring
Rinsing	4.5	Deionized water	3-10 s	RT	Mechanical stirring
Ag plating	0.5	Ag solution	Max. 10 min	RT	Mechanical stirring
Rinsing	4.5	Deionized water	3-10 s	RT	Mechanical stirring
Nickel	22.5	Ni solution	Max. 20 min	50-55°C	Magnetic stirring, 1-2 A (rectifier or DC), 2 anodes
Rinsing	4.5	Deionized water	3-10 s	RT	Mechanical stirring
Draining or drying	4.5	—	10 min	RT	—

RT, room temperature; Max., maximum; Min., minimum.

presents a scheme including details of each step of this process.

The following is the description of each of the steps, which can be applied to bamboo, wood, natural fibers, or any material made of cellulose.

1. Natural bamboo conditioning (cutting, cleaning, and dehydration). The bamboo was cut for preparing parquet, which in turn was cut in the shape and dimensions to be used in specific furniture or ornamental object. The bamboo should be cut from plants with an optimum age (above 7 yr) and dried to a humidity content less than 12%. The bamboo poles are obtained with lower water and carbohydrate levels by cutting them at dawn on a waning moon.
2. Preserving bamboo. The preserving methods prevent wood deterioration by fungi, termites, woodworm, and other xylophagous insects. The most common treatments include immersion for 5-8 h in a saline solution prepared with boric acid/borax/water ($H_3BO_3/Na_2B_4O_7 \cdot 10H_2O/H_2O$) at a ratio of 1:1:50. Another commonly used chemical treatment is mercerization, which consists of treating the natural fibers with a solution containing around 4% NaOH for 1 d, but the concentration is inversely proportional to the treatment time. Some chemical treatments use biodegradable pesticides with the specific function of preserving and protecting the bamboo against woodborers or xylophagous insects.
3. Bamboo dehydration. The humidity content in bamboo not only increases the risk of attack by fungi or insects, but also affects the layer deposition and its adherence. So, the wood pieces were introduced into an oven for drying at a temperature set in the range from 80 to 100°C. The drying time was from a minimum of 5 h to a maximum of 1 d.
4. Appling a lacquer. A lacquer was applied to protect or seal the bamboo and as a basis of

union between the bamboo and the next layer. The proportion of nitrocellulose lacquer to thinner was 1:1. The solution was applied with airbrushes, which provide uniform and thin covertures. The solution was applied three times with 5 min between each coating for air-drying. This stage can be carried out as well by deep-coating with immersion for a minimum of 3 s. Nevertheless, handling of pieces, solvent adsorption, and layer thicknesses were difficult to control.

5. Drying. The lacquer applied to the bamboo was dried at room temperature for 2-3 h. Alternatively, an oven preheated to 40°C can be used for half an hour. A moderate increment of temperature can reduce treatment times.
6. Application of colloidal copper paint. A similar procedure used for the lacquer was applied for the copper-containing solution.
7. Drying. The difference from the previous case is that it takes longer to dry.
8. Surface activation. The bamboo pieces were immersed in a solution of stannous chloride ($SnCl_2$)/HCl/de-ionized water for 5 min, with a back-and-forth motion. They were removed from the solution and drained for 5 s.
9. Rinse. The pieces were immersed in deionized water for 3-10 s with gentle agitation, then removed and drained for 3-5 s.
10. Electroless process for metallic silver. Different solutions were prepared to generate the plating, and the process consisted of the following: 1) silver nitrate saturated solution; 2) silver nitrate solution previously dissolved with ammonium hydroxide and potassium hydroxide. The solution exhibits an exothermic reaction before it was allowed to cool. 3) Ammonium hydroxide was added dropwise and under magnetic stirring until achieving the dissolution of the precipitates rich in silver. 4) To avoid an excess of ammonium hydroxide, a

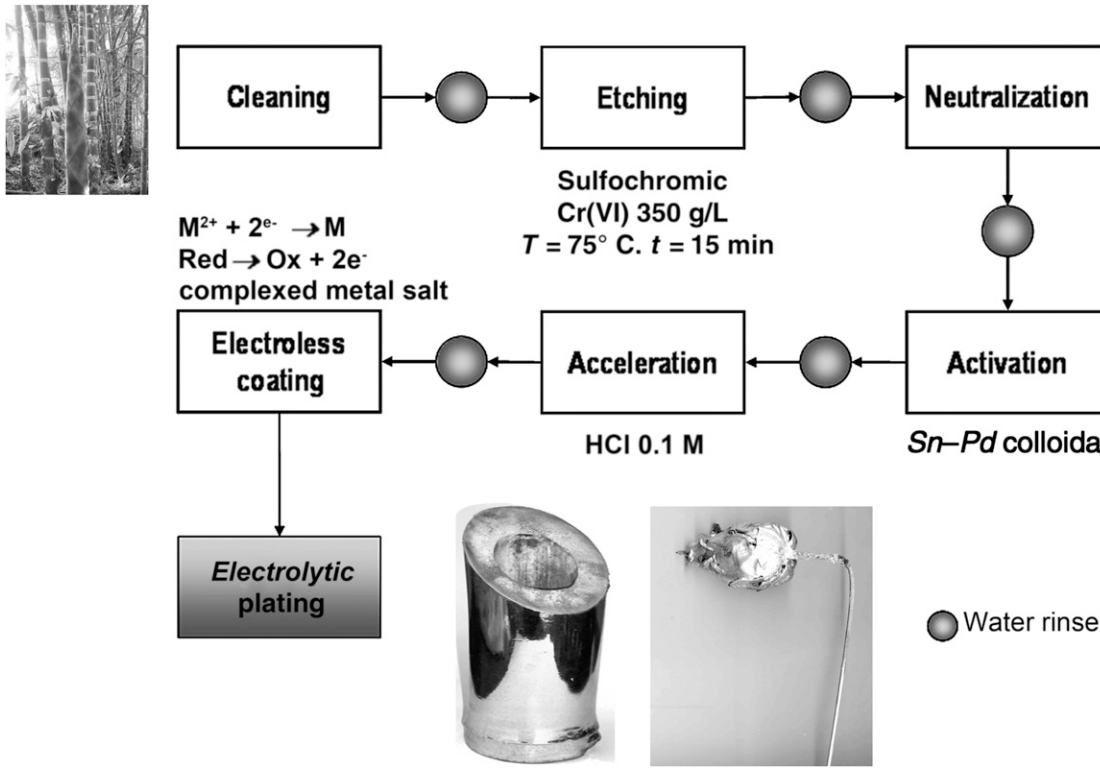

Figure 1. The sequence followed in the process for plating the nonconducting substrates. Two examples of finishing are shown: brass-coated bamboo and silver-coated rose.

saturated solution of silver was added until it obtained a pale yellow color. Moreover, a silver reducing solution was prepared, which contained sucrose (9%) and concentrated nitric acid (4 mL) in distilled water. The solution was boiled and cooled before use, with 20°C as the optimal working temperature. Later, the silver nitrate–ammonium hydroxide solution was mixed with the reducing solution at a 4:1 proportion. The bamboo pieces were completely covered by the solution. The pieces were maintained in the state for a maximum period of 10 min, after which the pieces were removed and allowed to drain. Thickness of the pieces was controlled by the immersion time or by controlling the silver nitrate concentration.

11. Rinse. The silvery bamboo pieces were immersed in deionized water for 3-10 s with gentle agitation, removed, and drained for 3-5 s.
12. Nickeling by an electrolytic process. Electrolytic nickeling was attained by using a nickel sulfamate, boric acid, and deionized water preparation. The silvery bamboo pieces were placed in an electrolytic cell in the cathode position. The setup consisted of two nickel anodes. The solution was heated maintaining a temperature in the range of 50-55°C under stirring. A current in the range of 1-2 A was applied with a Direct Current (DC) rectifier for a maximum time of 20 min.
13. Rinse. The nickel-plated bamboo pieces were immersed in deionized water for 3-10 s with gentle agitation, removed, and drained for 3-5 s.

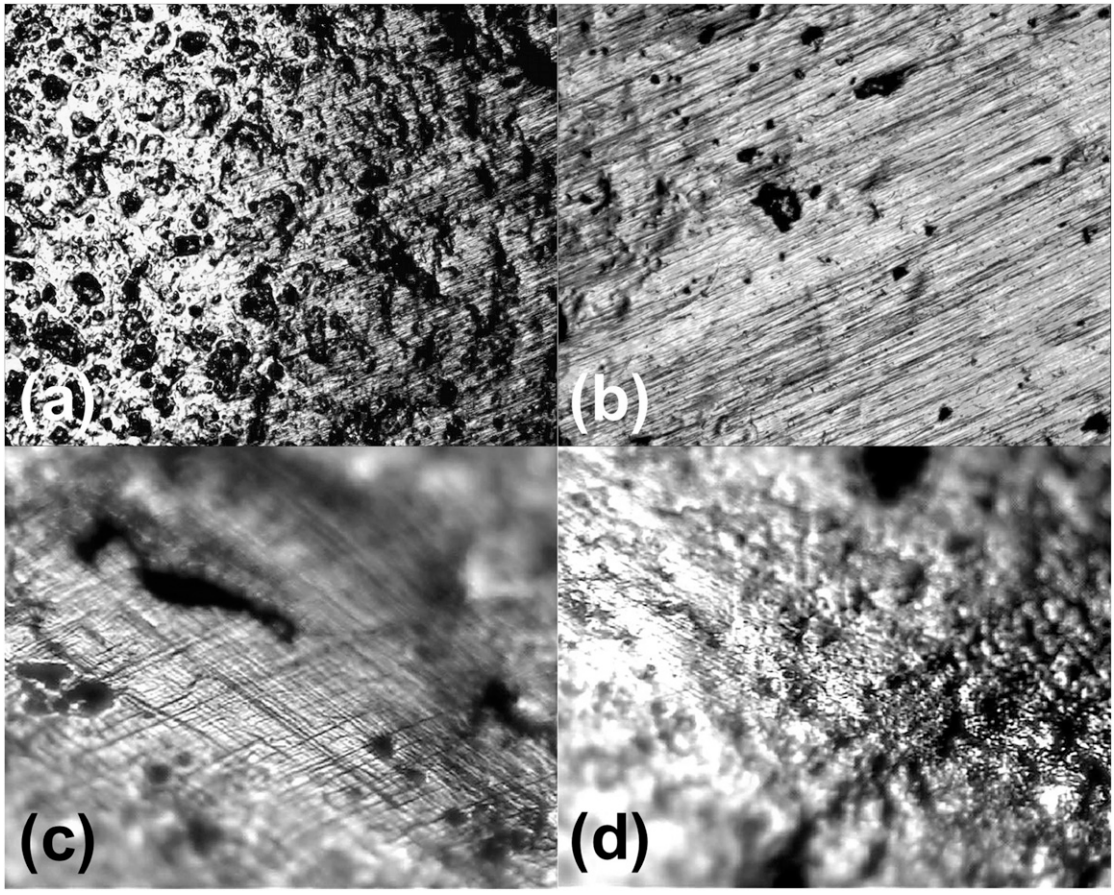

Figure 2. Optical micrographs showing evidence of wear as diagonal lines by Tabber tests (a) and (b). Different sites of abrasive rubber wheel path on the nickel-plated bamboo sample (c) and (d).

14. Drain and dry. The pieces were allowed to drain. Subsequently, hot air was applied with a dryer machine for 10 min.
15. Finally, the plated bamboo pieces were placed within different furniture designs.

The processes were exemplified above with the nickel-plating finishing, but many others have been applied and even more are viable by electroless and electrolytic procedures. Some examples of metal finishing surfaces are bright copper, antique or rustic copper, bright nickel, opaque nickel, black nickel, black silver, bright silver, gray zinc, bright yellow brass, dull yellow brass, bright tin, polished chrome, and other variations in appearance thereof.

Taber Abraser Model 5150 (TABER® Industries, North Tonawanda, NY) was used to conduct abrasion resistance tests on the coated pieces. The test was carried out using the CS10 abrasive rubber wheel (TABER® Industries) having a value of 88 in Shore A hardness, with a weight of 1000 g and a rotation speed of 70 rpm.

The Taber tests for abrasion resistance of the coatings were conducted according to the norm ASTM G195-08 (2013) and the norm ASTM D4060-10 (2013). A circular sample of parquet was prepared with a diameter of 10.8 cm and a centered hole of 0.6 cm, using 2-cm wide individual pieces. The circular piece of the parquet was treated for final nickel metallization. The test was stopped after 500 cycles and the sample was weighed. Thereafter, the test was resumed until completing 1000 cycles. The original weight was 39.7018 g, which reduced to 39.6839 g and subsequently to 39.6752 g, resulting in a final Taber wear index of 0.0266 by applying Eq 1.

$$I = \frac{(A-B)(1000)}{C}, \tag{1}$$

where I is the Taber wear index, A is the weight (mass) of the specimen before abrasion, B is the weight (mass) of the specimen after abrasion, and C is the number of test cycles.

$$I_1 = 39.7018 - 39.6839 \times 1000/500 = 0.0358,$$

$$I_2 = 39.6839 - 39.6752 \times 100/500 = 0.0174, \text{ and}$$

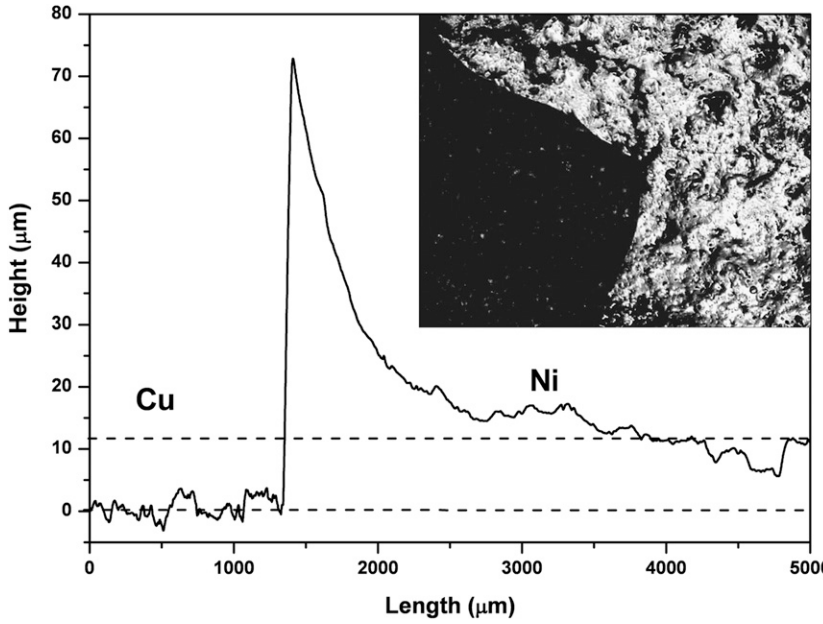

Figure 3. A profilometry graph of a segment between the nickel layer and copper sublayer obtained by making a triangular cut (dark area). The inset shows the micrograph of the segment used for measurement.

$I_3 = 39.7018 - 39.6752 \times 1000/1000 = 0.0266.$

Scanning Electronic Microscope (SEM) JEOL model 5400-LV (JEOL, Tokyo, Japan) was used to analyze the surface morphology of the plated bamboo pieces.

The reflectance spectra were measured using an USB2000+ Fiber Optic gated Ocean Optics

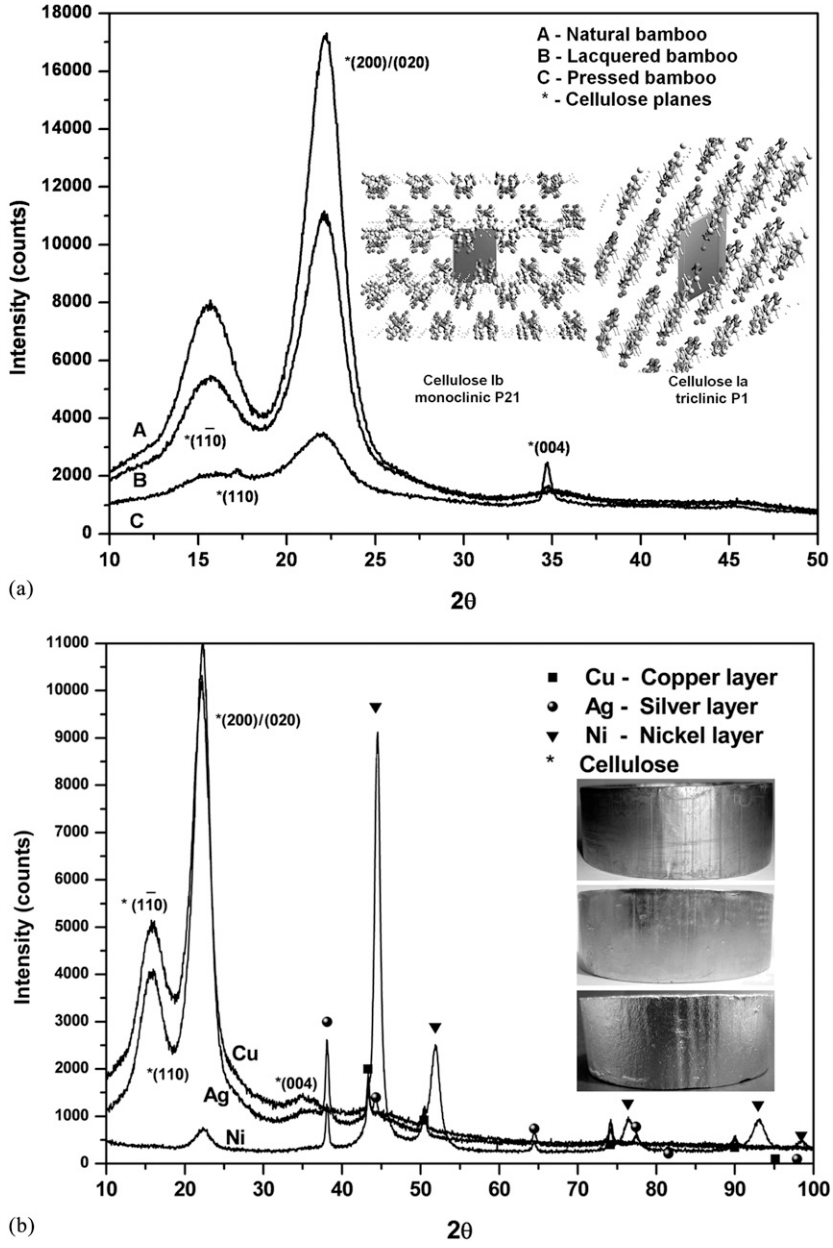

Figure 4. (a) X-ray diffractograms corresponding to three nonmetallized samples: polish bamboo, pressed bamboo, and lacquered bamboo. (b) Diffractograms corresponding to three metallic stages: Cu lacquer, Ag, and Ni. The two insets represent cellulose in its monoclinic and triclinic structures.

Table 2. Computed data from diffractograms of different analyzed samples corresponding to cellulose peaks and those for most intense peaks of Ni, Ag, and Cu.

Sample name		Observed max (2θ°)	Interplanar distance (nm)	Planes	Maximum intensity (Cps)	L (nm)	Full width at high maximum (2θ°)	Raw area (Cps × 2θ°)	Net area (Cps × 2θ°)
Ni plated	Ni	44.50	0.2034	(1 1 1)	3035	10.22 (10.0)	0.84	4349.4	3283
	Bamboo	22.28	0.3987	(2 0 0)	248	4.26	1.9	984.6	312.6
Ag plated	Ag	38.12	0.2359	(1 1 1)	867	17.88 (28.0)	0.47	2857.2	602.2
	Bamboo	22.32	0.3980	(2 0 0)	3672	3.58	2.26	12,760	7585.3
Cu painted	Cu	43.2	0.2092	(1 1 1)	522	21.91 (36.3)	0.39	477.2	59.36
	Bamboo	22.2	0.4001	(2 0 0)	3417	3.42	2.37	12,933.7	6346.2
Natural bamboo		15.65	0.5658	(1 $\bar{1}$ 0)	2681	—	2.76	11,382	4185.3
		22.24	0.3994	(2 0 0)	5760	3.46	2.34	19,354.7	11,881
		34.80	0.2576	(0 0 4)	498	—	2.44	2724.5	299.9
Compacted commercial		16.76	0.5285	(1 1 0)	892	—	a	5011.5	1347.3
bamboo ⊥ axial axis		21.82	0.4070	(2 0 0)	1336	2.34	3.46	6746.8	2459.7
		34.60	0.2590	(0 0 4)	606	—	0.10	704.5	8.922
Compacted commercial		17.22	0.5145	(1 1 0)	1072	—	0.26	921.3	53.54
bamboo ∥ axial axis		21.88	0.4059	(2 0 0)	1538	2.71	2.99	7135.8	2848.6
		34.69	0.2584	(0 0 4)	1523	—	0.41	1144.2	449.3

Cps, counts per second.
[a] Uncomputed data.

spectrometer (Ocean Optics, FL). The white references were Teflon™ and an aluminum thin film. The black reference was a cavity, self-constructed in the laboratory.

A Bruker AXS diffractometer (Bruker AXS, Karlsruhe, Germany) with CuKα_1 ($\lambda = 1.5406$ Å) radiation was used to conduct the crystalline characterization. The overall measurement conditions were as follows: scan speed 3 s/step, increment 0.04°2θ, 40 kV, 40 mA, soller slit, 0.6 mm slit, one scan. The TOPAS 4.2 software, and the AbsorbDX V. 1.1 and EVA V. 9.0 software of Bruker were used to analyze the diffractograms (Bruker AXS).

Roughness measurement was carried out using a Veeco Dektak 6M stylus profilometer (Veeco Instruments Inc., NY), with a pathway length of 5000 μm with a measurement time of 100 s using a diamond tip of 5 μm.

The proposed form for determining average roughness, quantifying the detected photons or counts of the (200) cellulose peak and considering the absorption of radiation, was

$$x = -\ln(1-p)\left(\mu(\lambda)\ \rho\left[\frac{1}{\sin\gamma} + \frac{1}{\sin(2\theta-\gamma)}\right]\right)^{-1}, \quad (2)$$

where x is the estimated depth, p is the % of contribution of the diffracted beam (μm), μ is the mass attenuation coefficient ($cm^2 \cdot g^{-1}$), ρ is the density of the material ($g \cdot cm^3$), γ is the angle between the incident beam and the surface, and 2θ is the deviation of the beam.

The diffractograms were collected by fixing the theta angle at 10° (X-ray source) and varying the detector position (2-theta).

The apparent value of the cross-sectional dimension L was calculated from the Scherrer equation (Newman 2008):

$$\tau = \frac{K\ \lambda}{\beta\ \cos\theta}. \quad (3)$$

Here, K is the dimensionless shape factor with a typical value of around 0.9; λ is the X-ray wavelength ($\lambda = 1.5406$ Å for CuKα_1); β is the full width at half maximum, expressed in radians of the peak corresponding to planes; and τ is the mean size of the ordered (crystalline) domains, which is limited to nanometric scale. The calculated crystallite size may be smaller than the grain size depending on crystalline defects, inhomogeneous strain, and instrumental effects, which contribute by broadening the peaks and reducing the value.

RESULTS AND DISCUSSION

Figure 1 describes the sequence followed for plating nonconducting substrates, specifically bamboo. The variation in the electroless process applied to plastics lies in applying lacquer to seal the porosity, obtruding the possible absorption of the plating solutions, which at the same time

Table 3. Thickness computed using ABSORB© and the quantified % of contribution to the diffractogram using TOPAS©.

		Lacquer/Cu/Ag		Lacquer/Cu/Ag/Ni		
	Lacquer/Cu	Cu	Ag	Cu	Ag	Ni
% (TOPAS©)	[a]	65.8	34.2	1.62	1.58	96.8
Weighted profile R-factor		—	13.79	—	—	12.187
direction	[a]	(1 1 1)	(1 1 1)	(1 1 1)	(1 1 1)	(1 1 1)
2θ°		43.298	38.116	43.298	38.116	44.5
E (keV) CuKα_1	[a]	8048	8048	8048	8048	8048
μ		50.92	212.1	50.92	212.1	46.13
μ_L		456.2	2227	456.2	2227	410.6
ρ (g/cm^3)		8.96	10.5	8.96	10.5	8.9
X (nm)	[a]	3103	278	47.23	9.1	11.140

[a] Uncomputed data (non-available signal).

Table 4. Thickness computed using ABSORB© and the quantified % of contribution to the diffractogram from the ratio of (element intensity)/(intensity of another element of the top layer, X_1) and of (element intensity)/(element intensity of another sample, X_2).

			Bamboo	Lacquer	Cu	Ag	Ni	
		X_1 (μm)	Max Int. (Cps)					X_2 (μm)
Bamboo sample			5760 100%	3706	3864	3885	255	
Lacquer sample			64.34%	No signal				
Cu sample	%	1.39	67.08% (382.57%)		1010 100%	1387	824	0.5
Ag sample		0.06 11	67.45% (252.76%)		137.33% (90.24%)	1537 100%	504	0.23 7
Ni sample			4.43% (6.6%)		81.58% (15.91)	32.79% (9.73%)	5180 100%	

would contaminate the wood, decreasing the chemical reagent concentration and increasing the cost. The sealing lacquer (organic solvent or water based) and the copper conducting lacquer were applied by spraying the surface with three layers each, which provides a thin homogeneous finishing. The next steps were the electroless/electrolytic process using stannous chloride ($SnCl_2$) as an activating agent for posterior metallization with silver and nickel, or other metals. Figure 1 shows two examples of finishing following the procedure described earlier: brass-coated bamboo and silver-coated rose.

The prepared nickel finishing using nickel sulfamate ($Ni(SO_3N_2)_2$) had a typical wear resistance, similar to a Watts solution (Saito et al 2007), which is around 26 mg loss/1000 cycles (Kanta et al 2009, 2010; Sahoo et al 2011; Brooman et al 2004). This result shows that the wear resistances achieved on bamboo were those already known for the finishing coatings according to their chemical composition and process conditions.

Figure 2(a) shows the darkened image of the abrasive rubber wheel path on the nickel-plated bamboo sample. The optical micrograph in Fig 2(b) presents an enlarged image of the area with the wear evident as diagonal lines. Figure 2(c) and (d) shows different sites on the worn path.

Figure 3 shows the profilometry graph of a segment between the nickel layer and copper sublayer obtained by a triangular cut (dark area). The inset shows the micrograph of the segment used for the measurement. The average roughnesses were 1.27 μm for the Cu layer and 1.17 μm for the Ni layer. The cut caused a bend in the nickel layer because of the internal stress, which had a thickness of around 12 nm (Fig 3). The nickel deposits had a highly uniform thickness and similar substrate roughness even at thick deposits. So, the final roughness greatly depended on the copper layer.

Because of the rough surface of the bamboo cuts, the thickness of each layer was difficult to measure. To analyze the metallic layers and obtain an average of their thicknesses in the illuminated area, X-ray diffraction was conducted in samples of each finishing: polish bamboo, pressed bamboo, lacquered bamboo, and Cu, Ag, and Ni layers. Figure 4(a) shows three of the diffractograms corresponding to nonmetallized samples. The peaks correspond to

cellulose in its monoclinic and triclinic structures with the family of planes identified. The two insets in Fig 4(a) represent structures with a size equal to three times the unitary cell in each axis. The unit cells are represented as the centered shadow areas.

The pressed bamboo shows an intensification of the peak corresponding to the 004 planes. This increase in crystallinity was identified perpendicular to the axial direction of the bamboo fibers. The tested samples showed a higher (004) peak around 10 ton/cm^2.

Figure 4(b) shows the other three diffractograms corresponding to metallized samples. The graphs correspond to a copper-lacquered sample, a succeeding silver-plated sample, and a sample with the final top nickel finishing. The cellulose signal decreased proportionally to the density and thickness of the layers.

Table 2 shows the different parameters associated with the diffractograms of each sample. The raw area of natural bamboo (200) planes was taken as reference. Comparatively, the Cu, Ag, and Ni subsequent layers reduce their raw area to

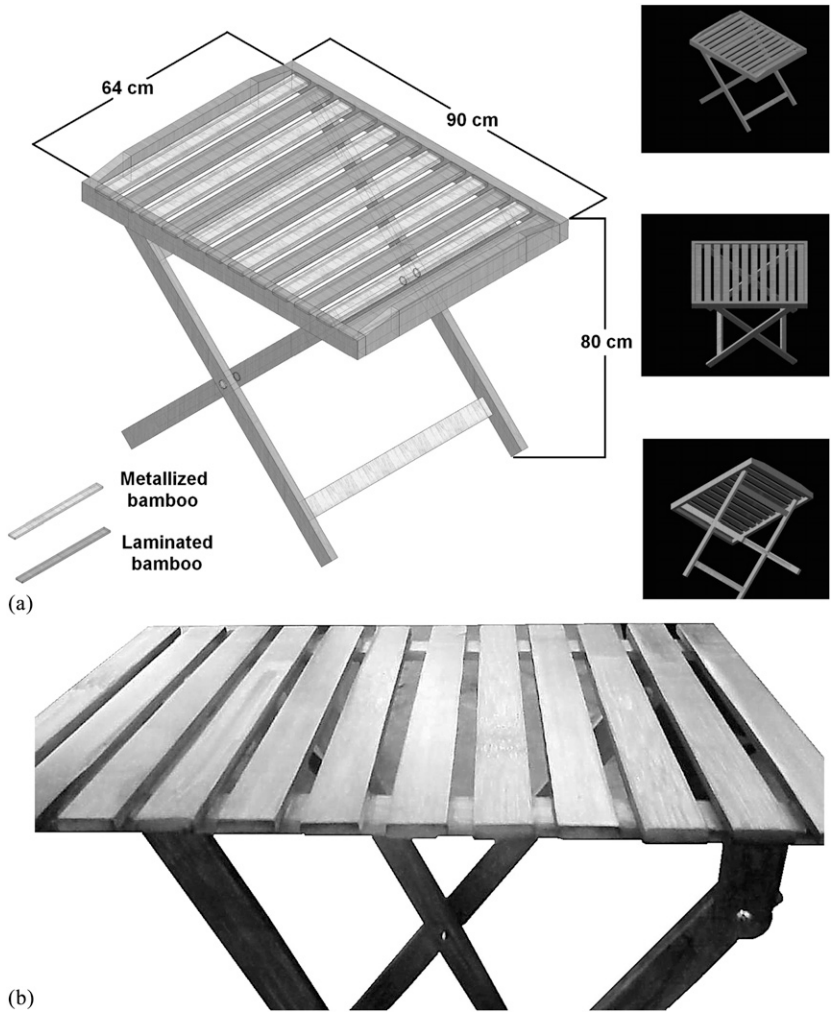

Figure 5. (a) Computer-Aided Design (CAD) image with a design for a bamboo parquet table. (b) A real model made with lacquered parquet.

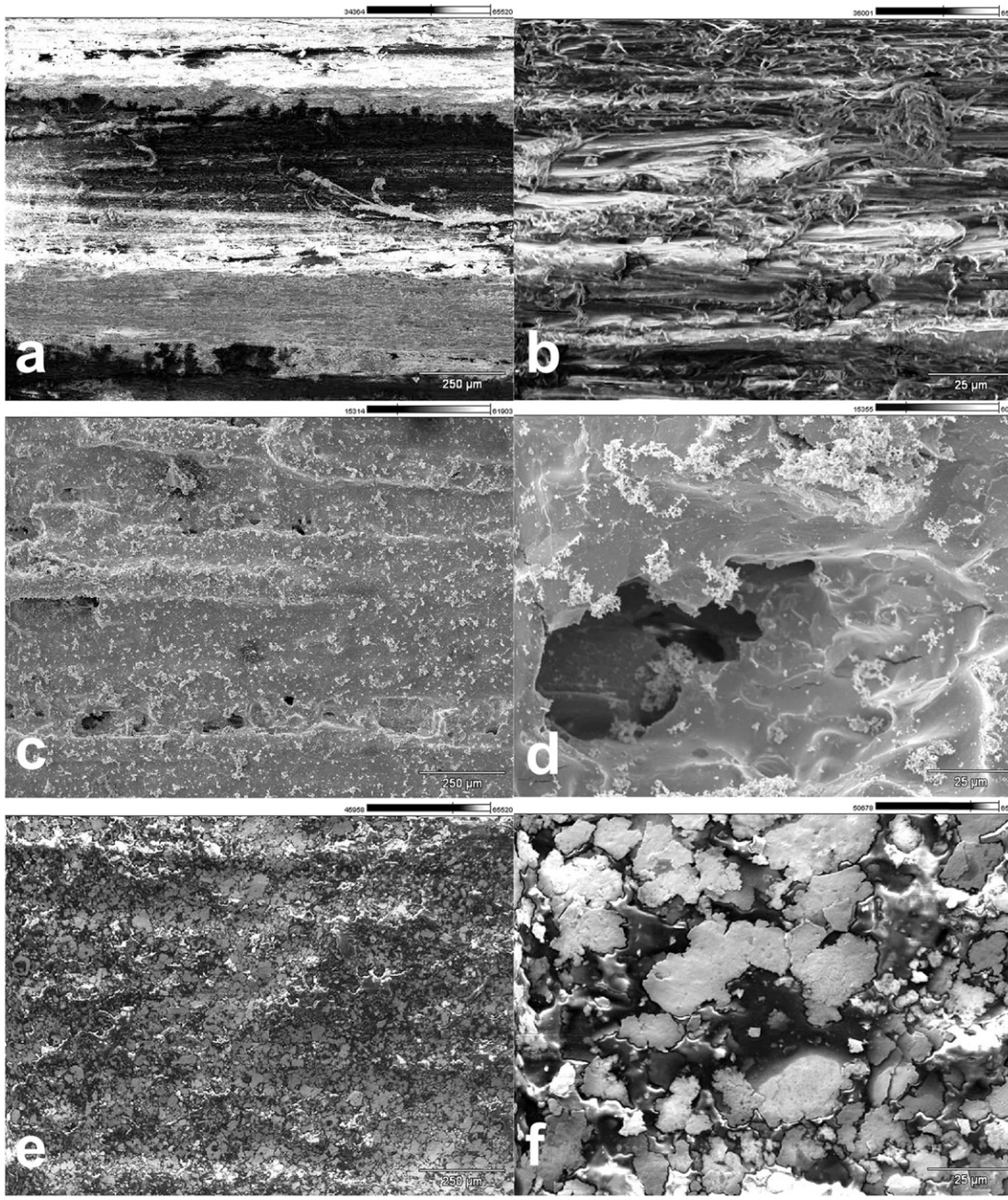

Figure 6. SEM images of bamboo parquet surfaces: (a) and (b) natural bamboo; (c) and (d) lacquer primer layer; (e) and (f) copper lacquer layer.

66.82%, 65.93%, and 5.01%, respectively. So, the attenuations caused by successive layers were around 33.18% with copper paint, 0.897% with silver plating (1.343%, attenuation relative to the previous layer), and 28.986% with nickel plating (7.72%, attenuation relative to the previous layer), relative to the raw area of bamboo (200) planes.

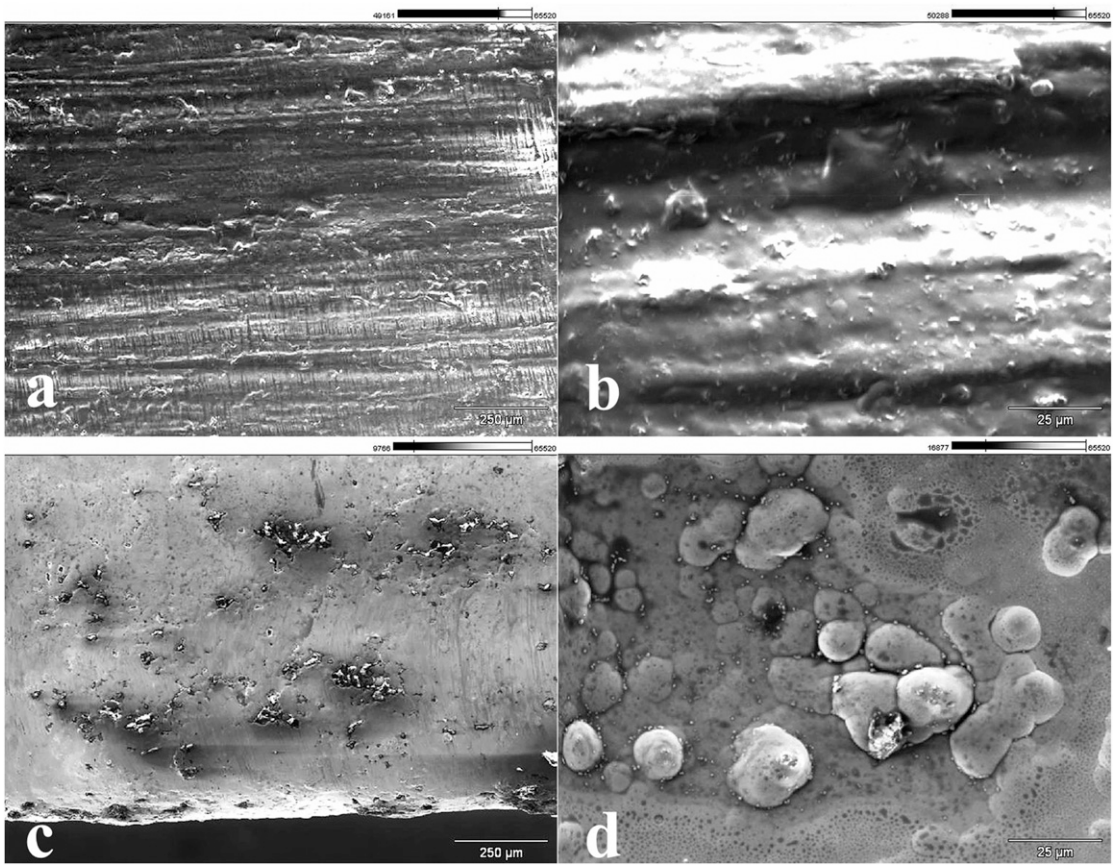

Figure 7. SEM images of bamboo parquet surfaces: (a) and (b) silver layer; (c) and (d) nickel finishing.

The intrinsic roughness of wood samples makes determining the average thickness of each metallic layer difficult. Tables 3-5 present the thickness measurement for each successive layer considering the peaks of the corresponding diffractograms for bamboo, Cu, Ag, and Ni. Table 3 shows the thickness of each layer computed using the software ABSORB© (Bruker AXS) and the quantified % of contribution to the diffractogram using TOPAS© (Bruker AXS). So, the computed thickness values were $X_{Cu} = 3.1$ µm and $X_{Ag} = 0.28$ µm, and $X_{Cu} = 0.047$ µm, $X_{Ag} = 0.009$ µm, and $X_{Ni} = 11.14$ µm.

Table 4 presents the percentage of attenuations between one layer and the subsequent layers shown below the diagonal line. In Table 4, the maximum intensity (counts per second) of the mean peak corresponding to each layer is shown above the diagonal line.

Figure 5 shows a folding table constructed with bamboo parquet. Figure 5(a) shows some design views, one main image and some from different perspectives. The main image presents the size and intercalation of metallized and varnished wood with an aesthetic finishing purpose. Figure 5(b) shows the table made of bamboo parquet. Metallized bamboo may be used in many different design concepts for furniture for both domestic and office use. Also, the bamboo flooring can include metallized finishing with varnish protection.

Figure 6 shows SEM micrographs corresponding to natural bamboo, Ag electroless, and Cu paint.

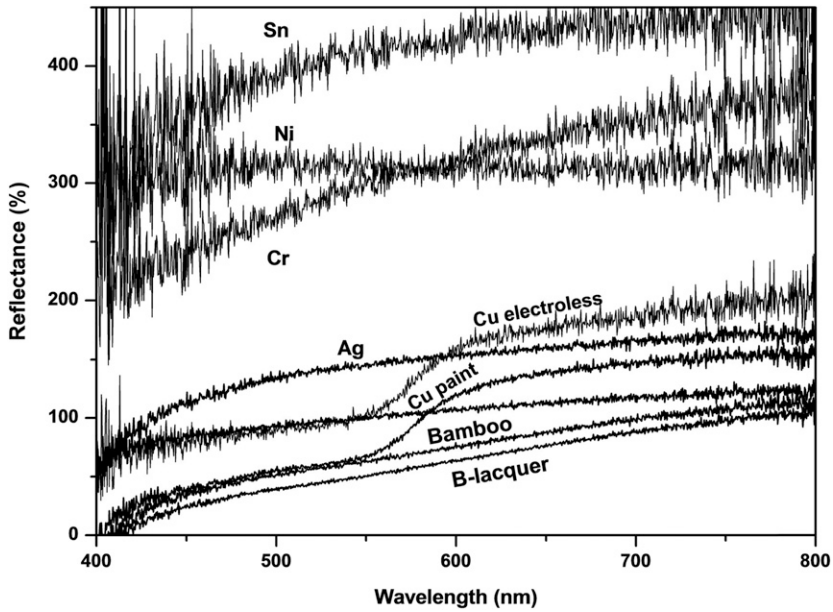

Figure 8. Reflectance spectra of different surface finishings: tin (Sn), nickel (Ni), chrome (Cr), silver (Ag), copper (Cu electroless), copper paint (Cu paint), natural bamboo (bamboo parquet), and varnished bamboo (B-lacquer).

The images in the left column were taken at 100× with a scalebar corresponding to 250 μm. The images in the right column were taken at 1000× with a scalebar corresponding to 25 μm. The natural bamboo images show a fibrous structure (Fig 6(a) and (b)). Figure 6(c) and (d) shows the coverture of most of these fibers with the Ag electroless layer, but the micrometric hole remained open. Also, there were some residues, fiber-like agglomerates on the surface but not strongly attached. Figure 6(e) and (f) shows the bamboo covered with a Cu paint, which contains Cu particles in an organic lacquer. This paint was included to compare with the electroless metallization. These micrographs show two types of zones, some lamellar plates surrounded by a matrix of lacquer. The paint, because of application with a paintbrush and the drying process, completely covers the wood surface. Nevertheless, the layer was not electrically conductive despite the high copper content.

Figure 7 shows the SEM micrographs corresponding to the primer lacquer layer and the Ni electroless top layer. The images in the left column were taken at 100× with a scalebar corresponding to 250 μm. The images in the right column were taken at 1000× with a scalebar corresponding to 25 μm. The applied lacquer layer resembles the surface finishing of the Cu

Table 5. Color parameters corresponding to different surfaces of bamboo samples.

Layer	*x*	*y*	*L**	*a**	*b**	Purity	$\lambda_{dominant}$
Sn	0.450	0.409	102.7	0.865	5.179	0.0780	547.3
Ni	0.467	0.413	101.6	4.9	13.4	0.175	587.7
Cr	0.442	0.408	101.0	−2.304	−2.000	0.0125	498.4
Ag	0.4671	0.4163	116.8	4	17.6	0.197	589.7
Cu electroless	0.442	0.408	98.7	−2.382	−2.310	0.0138	496.1
Cu paint	0.5305	0.4029	96.9	30.3	43.9	0.543	590.5
Bamboo parquet	0.4981	0.4191	86.6	11.8	31.5	0.431	586.7
B-lacquer	0.5081	0.419	80.3	13.9	35.3	0.5	586.1

lacquer, but homogenous and without the copper lamellar plates. Meanwhile, the electroless nickel top layer shows a continuous layer with some metallized holes. In a closer view within the holes, the Ni layer had some nodules attributed to the nucleation process of nickel or other previous metallic layers.

Figure 8 shows the reflectance spectra of the top of each studied layer. The graphs correspond to tin (Sn), nickel (Ni), chrome (Cr), silver (Ag), copper (Cu electroless), copper paint (Cu paint), natural bamboo (bamboo parquet), and varnished bamboo (B-lacquer). Some of these spectra are shown only for comparative purposes. Reflectance values above 100% are because of the difference between the metallic luster and the white reference, which corresponds to Teflon™ in the case of the graphs.

Table 5 presents the chromaticity diagram coordinates (a, y), CIE $L^*a^*b^*$ coordinates, color purity, and dominant wavelength. This characterization was carried out with the purpose of showing the quantitative values for the color of each surface. The values were obtained using an aluminum thin film as the white reference instead of Teflon™, which was used in the Fig 8 spectra. The differences in luster or luminosity, among the metallic surfaces and others, were observed. These surfaces were far from a mirror finishing because of the initial surface roughness and the lacquer used as a primer layer, but the metallic luster was that intended for decorative applications.

CONCLUSIONS

This work describes how bamboo was successfully plated with different metals and finishing. The coatings obtained include copper, silver, nickel, brass, and tin, each of which had some luster variations. The main change incorporated in the process for metallizing nonconducting surfaces was the introduction of a common base for all surfaces, regardless of its roughness, shape, size, or other surface conditions. Then, this base was taken through the electroless process, followed by electrolytic stages. Modification of the current process prevents the need for an initial etching stage for chemical conditioning and increasing roughness. The intrinsic roughness of wood samples makes determining the average thickness of each metallic layer difficult. This work proposes a methodology using X-ray diffraction and some qualitative and quantitative software to determine the thickness of irregular metallic layers such as those prepared in this study.

Differences in luster among the metallic surfaces and others were observed. These surfaces were far from a mirror finishing because of the initial surface roughness and the lacquer proposed as a primer layer, but the metallic luster was that intended for decorative applications.

ACKNOWLEDGMENTS

This work was carried out under the auspices of the Mexican Council for Science and Technology CONACYT, through the project CEMIE-Sol No. 207450 P18, P62, and P96; Graphenic Materials National Laboratory No. 293371. The authors thank the World Bank and the Energy Secretariat for the grant of the PRODETES Price, No. 002/2017/PRODETES-PLATA. Also, the first author acknowledges CONACYT for his graduate fellowship.

REFERENCES

ASTM G195-08 (2013) Standard guide for conducting wear tests using a rotary platform, double head abraser. Book of standards volume: 03.02. ASTM, West Conshohocken, PA.

ASTM D4060-10 (2013) Standard test method for abrasion resistance of organic coatings by the Taber abraser. Book of standards volume: 06.02. ASTM, West Conshohocken, PA.

Brooman EW (2004) Wear behavior of environmentally acceptable alternatives to chromium coatings: Nickel-based candidates. Met Finish 102:75-82.

Eichhorn SJ, Dufresne A, Aranguren M, Marcovich NE, Capadona JR, Rowan SJ, Weder C, Thielemans W, Roman M, Renneckar S, Gindl W, Veigel S, Keckes J, Yano H, Abe K, Nogi M, Nakagaito AN, Mangalam A, Simonsen J, Benight AS, Bismarck A, Berglund LA, Peijs T (2010) Review: Current international research into cellulose nanofibres and nanocomposites. J Mater Sci 45:1-33.

Hui B, Li J, Wang L (2014) Electromagnetic shielding wood-based composite from electroless plating corrosion-resistant Ni–Cu–P coatings on *Fraxinus mandshurica* veneer. Wood Sci Technol 48:961-979.

Kanta AF, Vitry V, Delaunois F (2009) Wear and corrosion resistance behaviors of autocatalytic electroless plating. J Alloys Compd 486:L21-L23.

Kanta AF, Vitry V, Delaunois F (2010) Wear and corrosion resistance of electroless nickel–boron coated mild steel. Mater Sci Forum 638-642:846-851.

Newman RH (2008) Simulation of X-ray diffractograms relevant to the purported polymorphs cellulose IVI and IVII. Cellulose 15:769-778.

Obataya E, Kitin P, Yamauchi H (2007) Bending characteristics of bamboo (*Phyllostachys pubescens*) with respect to its fiber–foam composite structure. Wood Sci Technol 41:385-400.

Sahoo P, Das SK (2011) Tribology of electroless nickel coatings—A review. Mater Des 32:1760-1775.

Saito F, Kishimoto K, Nobira Y, Kobayakawa K, Sato Y (2007) Nickel electroplating bath using malic acid as a substitute agent for boric acid. Met Finish 105:192-204.

Shi C, Tang Z, Wang L, Wang L (2017) Preparation and characterization of conductive and corrosion-resistant wood-based composite by electroless Ni–W–P plating on birch veneer. Wood Sci Technol 51:685-698.

Sittisart P, Hyland MM, Hodgson MA, Nguyen C, Fernyhough A (2014) Preparation and characterization of electroless nickel-coated cellulose fibres. Wood Sci Technol 48:841-853.

Sun L, Li J, Wang L (2012) Electromagnetic interference shielding material from electroless copper plating on birch veneer. Wood Sci Technol 46:1061-1071.

Wang L, Li J, Liu H (2011) A simple process for electroless plating nickel-phosphorus film on wood veneer. Wood Sci Technol 45:161-167.

Xing Y, Xue Y, Song J, Sun Y, Huang L, Liu X, Sun J (2018) Superhydrophobic coatings on wood substrate for self-cleaning and EMI shielding. Appl Surf Sci 436: 865-872.

Xing-yan H, Jin-qiu Q, Jiu-long X, Jian-feng H, Bai-dong Q, Si-min Ch (2015) Variation in anatomical characteristics of bamboo, *Bambusa rigida* (Variasi dalam ciri anatomi buluh, *Bambusa rigida*). Sains Malays 44:17-23.

Zhao WX, Ma Q, Li LS, Li XR, Wang ZL (2014) Surface modification of ABS by photocatalytic treatment for electroless copper plating. J Adhes Sci Technol 28: 499-511.

Zhao X, Chen H, Wang S, Wu Q, Xia N, Kong F (2018) Electroless decoration of cellulose paper with nickel nanoparticles: A hybrid carbon fiber for supercapacitors. Mater Chem Phys 215:157-162.